Insect Molecular Biology (2007) **16**(6), 661–674 doi: 10.1111/j.1365-2583.2007.00762.x

Hepatopancreatic multi-transcript expression patterns in the crayfish *Cherax quadricarinatus* during the moult cycle

Y. Yudkovski*, A. Shechter†‡, V. Chalifa-Caspi‡, M. Auslander*§, R. Ophir¶, C. Dauphin-Villemant, M. Waterman††, A. Sagi†‡ and M. Tom***

**Israel Oceanographic and Limnological Research, Haifa, Israel;* †*Department of Life Sciences and the* ‡*National Institute for Biotechnology in the Negev, Ben-Gurion University of the Negev, Beer Sheva, Israel;* §*Faculty of Civil and Environmental Engineering, Technion-Israel Institute of Technology, Technion City, Haifa, Israel;* ¶*Weizmann Institute of Science, Rehovot, Israel;* ***FRE2852 CNRS-UPMC, Laboratoire Protéines Biochimie structurale et fonctionnelle, Paris, France; and* ††*Vanderbilt University, School of Medicine, Nashville, TN, USA*

Abstract

Alterations of hepatopancreatic multi-transcript expression patterns, related to induced moult cycle, were identified in male *Cherax quadricarinatus* through cDNA microarray hybridizations of hepatopancreatic transcript populations. Moult was induced by X–organ sinus gland extirpation or by repeated injections of 20-hydroxyecdysone. Manipulated males were sacrificed at premoult or early postmoult, and a reference population was sacrificed at intermoult. Differentially expressed genes among the four combinations of two induction methods and two moult stages were identified. Biologically interesting clusters revealing concurrently changing transcript expressions across treatments were selected, characterized by a general shift of expression throughout premoult and early postmoult vs. intermoult, or by different premoult vs. postmoult expressions. A number of genes were differentially expressed in 20-hydroxyecdysone-injected crayfish vs. X–organ sinus gland extirpated males.

Keywords: crustaceans, ecdysteroids, moult cycle, hepatopancreas, cDNA microarray.

Introduction

Crustacean growth and development is a stepwise process depending on a periodic shedding of the four-layered, rigid a-cellular cuticle. The shedding event, termed ecdysis, is part of the complex and prolonged moult cycle that comprises four stages: premoult, ecdysis, postmoult, and intermoult (Skinner, 1962, 1985; Aiken & Waddy, 1987; Chang, 1991, 1995). Premoult entails separation of the old cuticle from the underlying hypodermis (apolysis) via cuticle digestion and the concurrent secretion of a new exocuticle and epicuticle. The onset of premoult is accompanied by increased circulatory glucose and lipids, either mobilized from hepatopancreatic deposits or degraded from the old cuticle. Freshwater crayfish inhabiting calcium-deficient habitats save calcium by its mobilization from the old cuticle and its deposition in button-like calcium carbonate structures, termed gastroliths, located beneath the gastric epithelium. Ecdysis is driven by the active absorption of water to increase the body's volume, leading to rupture of the partly degraded old cuticle, after which the now larger individual emerges enveloped in the new cuticle. Postmoult is characterized by endocuticle and membranous layer formation and gradual replacement of the absorbed water by tissues. At postmoult, the gastroliths collapse into the stomach and dissolve, and the calcium is mobilized to the new cuticle, rendering it more rigid. Intermoult is characterized by very low moult-related metabolic activity and no structures connected with moulting.

The crustacean moult cycle is controlled by multiple factors, including hormones. Ecdysteroids, the moulting hormones common to all arthropods, are synthesized in the crustacean Y-organs, endocrine steroidogenic glands of ectodermal origin (reviewed in Lachaise *et al.*, 1993). The increase in ecdysteroid synthesis at the onset of premoult

Received 29 March 2007; accepted after revision 29 June 2007; first published online 19 October 2007. Correspondence: Dr. Moshe Tom, Israel Oceanographic and Limnological Research, P.O.B. 8030, Haifa 31080, Israel. Tel.: + 972 4 8565 257; fax: + 972 4 8511 911; e-mail: tom@ocean.org.il; moshetom@netvision.net.il

Present Address (Dr. R. Ophir): Agricultural Research Organization of Israel, Volcani Center, Plant sciences, P.O.B. 6, Bet Dagan, 50250, Israel.

leads to a surge of circulating 20-hydroxyecdysone (20E) that triggers a programmed synthesis of proteins in the epidermis and the hepatopancreas (Bielefeld *et al*., 1986; Traub *et al*., 1987; Stringfellow & Skinner, 1988). For successful ecdysis, a decrease in the 20E level is required immediately prior to moulting; without this drop ecdysis is delayed (Chang *et al*., 1993).

Y-organ activity is under complex control (Lachaise *et al*., 1993) that is not yet completely understood. One of the better understood effectors is the neuropeptidic moult-inhibiting hormone (MIH), which is secreted from the neurosecretory X-organ sinus gland (XO-SG) complex, located in the crustacean eyestalk (Keller, 1992). Production of MIH causes the level of circulating ecdysteroids to fall. At premoult or following XO-SG extirpation, reduced MIH secretion releases this inhibition, thus enabling ecdysteroid synthesis and the onset of premoult (reviewed in Chang *et al*., 1993). The subsequent decrease in the secretion of ecdysteroids prior to moult is directly affected by circulating 20E and indirectly by the stimulatory effect of 20E on X-organ secretion (reviewed in Dell *et al*., 1999).

Crustacean moult and reproduction take place throughout the adult life cycle, with the different stages being coordinated to be sequential or simultaneously occurring processes, depending on the biology of the species (Nelson, 1991). For *Cherax quadricarinatus*, the present experimental species, these events appear to be sequential (Barki *et al*., 1997). *Cherax quadricarinatus* ovarian development, including intensive hepatopancreatic synthesis of vitellogenin, the egg yolk precursor, is induced by XO-SG extirpation (Abdu *et al*., 2002).

Moulting is common to all arthropods. In insects it occurs during the larval growth and pupal stages as part of the complex insect metamorphosis. In contrast, most crustaceans continue both to grow and to moult during adulthood, but at this phase of their life cycle it is a simpler process, presumably related mainly to absorption of the old cuticle, formation of a new one, and growth. As crustaceans are a more ancient group than insects in evolutionary terms (Glenner *et al*., 2007), the simple moulting process, not masked by more complex developmental events, may enable the identification of strictly moult-related genes, which may have acquired more diversified functions later during arthropod evolution. Because the complex moult cycle is characterized by dramatic changes in multi-gene expression patterns in several organs, the cDNA microarray is an efficient methodology to evaluate these patterns and their relationships to biological situations.

Insect developmental multi-gene expression patterns, which include repeated moult cycles, have been studied in several species (White *et al*., 1999; Arbeitman *et al*., 2002; Ote *et al*., 2004; Beckstead *et al*., 2005; Goodisman *et al*., 2005). A number of studies have examined crustacean multi-gene expression patterns using cDNA microarray (Dhar *et al*., 2003; Soetaert *et al*., 2006; Stepanyan *et al*., 2006; Stillman *et al*., 2006), but none has focused on the moult cycle. Hence, the present study was aimed at elucidating hepatopancreatic gene expression patterns and their changes during crustacean moult cycle.

The moult cycle of our experimental species, the crayfish *C. quadricarinatus*, was induced by the broadly-affecting removal of the XO-SG complex or by repeated 20E injections targeted directly at moult induction. Moult stages were identified by an accurate three-parameter moult-staging system. The methodologies of both moult induction and moult-staging in *C. quadricarinatus* were developed by the companion study of Shechter *et al*. (2007), and are briefly described below ('Experimental procedures' section). Multi-gene expression patterns were characterized by using a *C. quadricarinatus* cDNA microarray, which was constructed as part of the present study.

Results

Characteristics of the microarray cDNA assemblage

The term 'clone' in this article means single cloned DNA fragment, printed in duplicate spots on the microarray. The term 'unique clone' is used to describe a consensus sequence constructed by the assembly of several identical clone sequences, fully or partially overlapping. Each unique clone was deposited in GenBank, receiving an identifying accession number.

The microarray was constructed from 4800 partial cDNAs, cloned from *C. quadricarinatus* hepatopancreas, epidermis and Y organ. A subset of clones was sequenced, and 516 adequate unique clones (> 50 bp) out of 1082 successfully sequenced clones, were deposited in GenBank (accession numbers DQ847528–DQ847992; EF426494–EF426497; EF692582–EF692629). Sequencing was performed mainly with differentially expressed clones resulted from the moult induction experiment (see below). These sequences included nine ribosomal RNA unique clones and nine unique clones that originated from spiked yeast clones added to the assemblage as controls and not used in the present analysis. From the deposited sequences, 504 were present in 1–10 copy numbers, whereas 12 were present in 11–93 copies. The statistics of the sequenced clones reflected a whole library estimate of 2289 unique clones, 429 of which were ribosomal RNA and external spiked controls, leaving around 1860 unique transcript sequences. The DNA length in the assemblage averaged 412 ± 234 bp.

Construction of the cDNA assemblage was carried out using the SMART-SSH methodology, designed to preferentially clone from the target tissue differentially expressed genes, in comparison to a reference cDNA. The reference cDNA produced from *C. quadricarinatus* muscle (see Experimental procedures). The SMART-SSH approach was aimed at roughly equalizing the representation of

Table 1. Characterization of *Cherax quadricarinatus* experimental groups

Treatment group	No. of males	Average weight (g)	Average MMI	No. of days after moult induction	Setae development index at sacrifice	Circulating ecdysteroids (20E) at sacrifice (pg/µl)
Intermoult (Ref1)	6	30.6	0	0	C	4.8 ± 1.05
Intermoult (Ref2)	3	31.4	0	0	C	3.8 ± 0.95
Intermoult (Ref3)	3	33.7	0	0	C	5.2 ± 1.1
Injected–sacrificed at premoult	3	32.2	0.09	10	D_2	1076 ± 79
Injected–sacrificed 1 day after moult	3	35.5	0.11	14–16	A	28 ± 3.8
Extirpated–sacrificed at premoult	3	25.4	0.09	8	D_{1-2}	534 ± 25
Extirpated–sacrificed 1 day after moult	3	24.4	0.11	11–12	A	16.1 ± 1.9

MMI, moult mineralization index (gastrolith width/carapace length). Setae development index designations: C, intermoult; D_{1-2}, premoult stages; A, initial postmoult. Moult staging methodology and terms are detailed in Shechter *et al.* (2007).

cDNAs in the constructed assemblage and also at minimizing ribosomal RNA clones. The constructed library, with about 53% redundancy, did not reach the optimal equalization. In addition, ribosomal RNAs, composing 17% of the library, were not entirely eliminated. When control spiked clones (1.9%) are added to this percentage, the estimated percentage of unusable spots is 18.9%. The microarray platform was deposited in the Gene expression omnibus (GEO) database maintained by the American National Center for Biotechnology Information (NCBI). (platform accession number GPL4786).

Moult induction experiment

To avoid interference from gene expression patterns related to ovarian development, only males were used for the induction experiment. The study population comprised 24 intermoult males divided into seven groups, i.e., six groups of three crayfish each and one group of six crayfish. The six-male group and two three-male groups served as the three nontreated reference intermoult groups. Hepatopancreatic RNA from the animals in each of these groups was pooled. The moult cycle was induced in two of the treatment groups by extirpation of the XO-SG complex and in two other treatment groups via repeated injections of 20E. The animals of one group of each treatment were sacrificed at premoult, and those of the other group, a day after moult. In total, five experimental conditions were examined: intermoult reference (Ref), injected-premoult (Ipre), injected-postmoult (Ipost), extirpated-premoult (Epre), and extirpated-postmoult (Epost). Experimental design and staging parameters are presented in Table 1. Hepatopancreatic RNAs extracted from the animals upon termination of the experiment were converted to cDNAs, labelled and hybridized on the microarray slides. The hybridization design included dual hybridizations between each treatment and the reference as well as among the treatments. Differential expression of genes between the three reference groups was examined by a smaller set of hybridizations (see detailed hybridization design and analysis in Fig. 1 and in 'Experimental procedures' below).

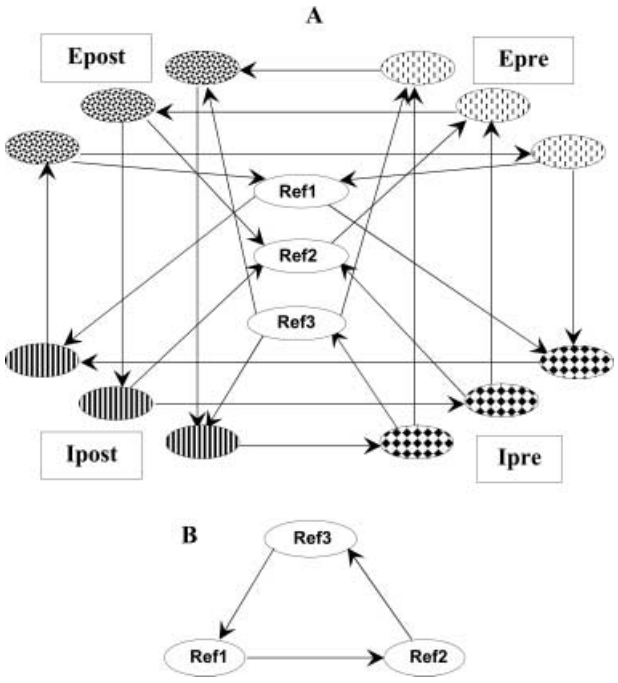

Figure 1. Hybridization designs. (A) Multiple comparisons among the experimental conditions and the reference pools. (B) Hybridization design for assessing differential expression among the three reference pools. Ellipses designate single males at four combinations of moult stage and moult measure of induction or pools of three to six intermoult reference males (see Results and Table 2 legend for abbreviations of experimental conditions). Each arrow connects two RNA populations hybridized onto one slide. Arrowhead – Cy3 labelling, tail – Cy5 labelling. Alternate arrow directions were used in different biological replicates to compensate for putative dye effects.

Clustering and cluster characteristics

By using *LIMMA* software (see 'Experimental procedures'), $\log_2$ expression ratios (*M*) of each clone were calculated for eight selected binary comparisons of pairs of experimental conditions, resulting in an *M*-profile composed of eight values for each clone. The first four binary comparisons represented treatment vs. reference *M*-values, as follows: (1) Epre vs. Ref; (2) Ipre vs. Ref. (3) Epost vs. Ref; and (4)

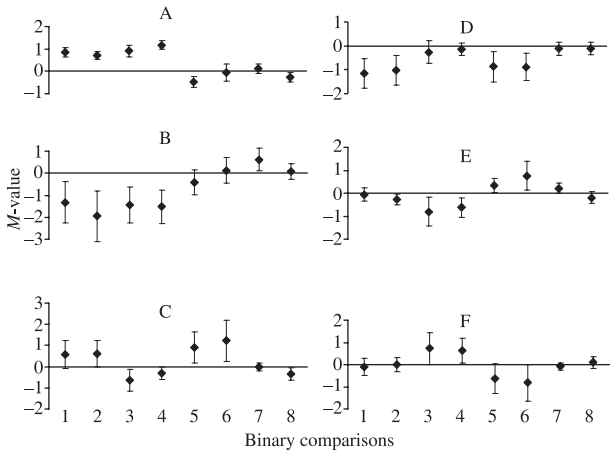

Figure 2. Clustering results. Selected clusters (A–F) of similarly expressed genes across the experiment. The *x*-axis represents binary comparisons between pairs of experimental conditions: 1, Epre–Ref; 2, Ipre–Ref; 3, Epost–Ref; 4, Ipost–Ref; 5, Ipre–Ipost; 6, Epre–Epost; 7, Epre–Ipre; 8, Epost–Ipost. (See Results and Table 2 legend for abbreviations of experimental conditions.) Each point represents the average *M*-value of all unique clones participating in the cluster and their standard deviations.

Ipost vs. Ref. The other four *M* profiles represented inter-treatment comparisons: (5) Ipre vs. Ipost; (6) Epre vs. Epost; (7) Epre vs. Ipre; and (8) Epost vs. Ipost. *LIMMA* also distinguished the statistically significant differential expressions ($M \neq 0$).

Clones revealing low average fluorescent intensity across the experiment and also ribosomal RNA and spiked yeast clones, were excluded from the analysis. The *M*-profiles of the remaining 1865 clones were subjected to cluster analysis performed with *EXPANDER* software using *Click*, *K-means* and *SOM* algorithms, applying several alternate algorithm-related parameters for each of the algorithms. The selected binary comparisons were aimed at revealing differences of gene expression patterns between premoult and intermoult, postmoult and intermoult, premoult and postmoult and between the two measures of moult induction. Six biologically interesting clusters responding to the experimental aims were selected. Two of them (Fig. 2A,B) were formed by *K-means* with six predetermined groups, and the other four (Fig. 2C–F) were formed by *Click* with a predetermined homogeneity of 0.85.

Gene-related information, arranged according to the selected clusters, is detailed in Tables 2–7. For each unique clone, the GenBank accession number and BLAST and Gene Ontology (GO) annotations are given. Several unique clones were present in multiple clusters, and the total number of their clones on the array and in each cluster is provided. Cluster-related statistics included the total number of clones, the number of nonsequenced clones, the total number of differentially-expressed clones (DEC) in at least one of the binary comparisons, and the number of differentially expressed clones for each binary comparison and their average *M*-values. Several spots belonging to clusters B and C revealed differential expression in reference 2 and/or 3 in relation to reference 1, and their respective numbers in each cluster are provided. The six clusters contained a total of 299 unique clones. However, the sequencing of 46 of them failed and is missing.

Three moult-related gene expression patterns were identified in the hepatopancreas in relation to the conditions examined, using our set of cDNAs: (1) the mirror-imaged clusters A and B elucidated a general shift in the hepatopancreatic expression pattern at the onset of premoult, which lasted through premoult and early postmoult, in comparison with the intermoult status. The clones of cluster A were induced, whereas those of cluster B were attenuated (Fig. 2A,B, binary comparisons 1–4; Tables 2 and 3, entries depicting number of DEC of Epre–Ref, Ipre–Ref, Epost–Ref and Ipost–Ref and their average *M*-values); (2) the genes comprising clusters C–F elucidated moult stage-related expression patterns, which were altered during the premoult–postmoult transition (Fig. 2C–F, binary comparisons 1–4; Tables 4–7, entries depicting the number of DEC of Epre–Ref, Ipre–Ref, Epost–Ref and Ipost–Ref and their average *M*-values). C and E are mirror images of D and F, respectively and the former two revealed higher levels at premoult, and the latter at postmoult; (3) no cluster revealed differences between the two measures of induction, 20E injections and XO-SG extirpation. Hence, binary comparisons between the two treatments in both premoult and postmoult elucidated *M*-values close to zero (Fig. 2A–F, binary comparisons 7 and 8 and Tables 2 and 4–7, entries depicting number of DEC of Epre–Ipre and Epost–Ipost). However, 33 differentially expressed clones were observed in cluster B upon comparison of premoult injected and extirpated males (Table 3, entries depicting number of DEC of Epre–Ipre). The 18 accession numbers assigned to these clones are highlighted in Table 3.

Binary comparisons of the three references revealed almost no differences in clusters A and C–F (Tables 2 and 4–7, entries depicting number of DEC comparing ref2 and ref3 to ref1). The expression patterns of the references are slightly more variable in cluster B (Table 3, entries depicting number of DEC comparing ref2 and ref3 to ref1). However, even in cluster B, these differences were assigned only to 10 unique clones out of 154, and it can be concluded that the three reference samples are uniform, permitting sensitive distinction of significant differential expression because of treatment and moult stage. The supplementary data from the *LIMMA* analysis were deposited in the NCBI-GEO database (series accession no. GSE6947).

A number of unique clones of cysteine proteinases (accession no.: DQ847633; DQ847637; DQ847745; DQ847747; DQ847749) were present in both clusters A

Table 2. Characteristics of cluster A constructed of *M*-value profiles across eight binary comparisons of experimental conditions

Accession number	Sequence annotation	GO terms summary	Seq. clones	In cluster
DQ847633	Cysteine proteinase preproenzyme	Cathepsin L	39	1
DQ847637	Cysteine proteinase preproenzyme	Cathepsin L	14	2
DQ847745	Digestive cysteine proteinase 3	Cathepsin L	4	1
DQ847747	Digestive cysteine proteinase 1	Cathepsin L	2	1
DQ847749	Digestive cysteine proteinase 1	Cathepsin L	16	2
DQ847584	Cathepsin C isoform 1	Dipeptidyl-peptidase I		
DQ847722	Kazal-type proteinase inhibitor	Serine-type endopeptidase inhibitor		
DQ847773	Glutamine synthetase			
DQ847585	Glutamine synthetase			
DQ847915	Arginine kinase			
DQ847724	Triacylglycerol lipase	Lipid metabolism	11	2
DQ847971	Beta 1,4-endoglucanase	Cellulase	1	1
DQ847757	ENSANGP00000021035-like	Peritrophic membrane chitin binding protein	2	1
DQ847592	Dehydrogenase; short chain family member (dhs-25)			
DQ847786	NADH dehydrogenase subunit 4	Mitochondrial NADH dehydrogenase (ubiquinone)		
DQ847586	Haemocyanin	Oxygen transporter	13	2
DQ847688	Haemocyanin 2	Oxygen transporter	13	8
DQ847704	Pseudohaemocyanin (PHc-1)		12	1
DQ847943	40S ribosomal protein S21	Structural constituent of ribosome		
DQ847655	*Cherax destructor* mitochondrion genome			
DQ847687	PREDICTED: similar to B52 CG10851-PB; isoform B	Nucleic acid binding		
DQ847811	Carcinin-like protein			
DQ847934	70kD heat shock-like protein			
DQ847938	PREDICTED: similar to CG6877-PA			
DQ847664	(Q6G288) Hypothetical protein			
DQ847636	K02F3.6			
DQ847689	(Q8WTI6) PFTAIRE-interacting factor 2 (CG31483-PA)		3	1
DQ847930	Alpha-III tubulin	Microtubule		
DQ847952	*Cherax quadricarinatus* microsatellite cqu.007 sequence			
EF426496	LEA dehydrin-like protein		3	1

Accession nos. of non-annotated unique clones: DQ847529; DQ847532; DQ847533; DQ847535; DQ847536; DQ847539; DQ847542; DQ847543; DQ847544; DQ847568; DQ847572;DQ847611; DQ847625; DQ847643; DQ847648; DQ847656; DQ847657; DQ847658; DQ847659; DQ847660; DQ847661; DQ847664; DQ847665; DQ847670; DQ847674; DQ847677; DQ847678; DQ847684; DQ847686; DQ847708; DQ847710; DQ847712; DQ847716; DQ847725; DQ847727; DQ847744; DQ847751; DQ847758; DQ847760; DQ847761; DQ847762; DQ847763; DQ847768; DQ847773; DQ847776; DQ847780; DQ847785; DQ847787; DQ847790; DQ847791; DQ847812; DQ847813; DQ847819; DQ847860; DQ847865; DQ847921; DQ847926; DQ847928; DQ847929; DQ847931; DQ847932; DQ847934; DQ847935; DQ847936; DQ847940; DQ847941; DQ847964; DQ847966; DQ847974; DQ847979; DQ847980; DQ847982; DQ847983; DQ847985; EF426494; EF426495; EF692596; EF692611; EF692621

136 clones in cluster A, five of them were not sequenced — 111 unique clones in cluster A

	Total DEC	Epre–Ref	Ipre–Ref	Epost–Ref	Ipost–Ref	Ipre–Ipost	Epre–Epost	Epre–Ipre	Epost–Ipost	ref 2–1	ref 3–1
DEC	119	25	7	33	114	3	3				
Ave. *M* of DEC		1.09 ± 0.19	1.05 ± 0.24	1.11 ± 0.43	1.20 ± 0.2	–1.53 ± 0.51	–2.16 ± 0.59				

Tables 2–7: Each unique clone (= accession number) is characterized by its BLAST and GO annotations where available. Several unique clones were present in a number of clusters, and their total number in the entire array (seq. clones column) and in each cluster (in cluster column), are provided. Clone-specific statistics for each cluster (lower part of each table) include the total number of clones, the number of nonsequenced clones, the number of unique clones, the total number of clones differentially expressed in at least one binary comparison (total DEC) and the number of differentially expressed clones for each binary comparison and their average *M*-values. Several clones belonging to clusters B and C revealed differential expression in references 2 and/or 3 in relation to reference 1, and their numbers in each cluster are provided. Ref, intermoult males; Epre, extirpated XO-SG males, sacrificed at premoult; Epost, extirpated XO-SG males, sacrificed at postmoult; Ipre, 20E-injected males, sacrificed at premoult; Ipost, 20E-injected males sacrificed at postmoult.

and B (Tables 2 and 3), apparently in a conflicting manner, as these two clusters are mirror images of one another. There were 75 clones belonging to these five unique clones, 60 of which were identified in cluster B and only seven in cluster A. Moreover, additional unique cysteine proteinase sequences (DQ847582; DQ847591; DQ847755; DQ847948) were present only in cluster B, and only one in cluster A (DQ847584). Therefore, almost all cysteine proteinases are assumed to genuinely belong to cluster B, reduced at the onset of premoult. In view of their annotations, these proteinases putatively belong to more than one gene (Le Boulay *et al*., 1995).

One beta 1,4-endoglucanase sequence (DQ847971) was displayed at one clone each, in clusters A and D, whereas another four unique clones of the same annotation (DQ847606; DQ847628; DQ847699; DQ847700) were evident at seven out of nine clones in cluster B. However, in view of BLAST comparisons (results not shown), not all of

Table 3. Characteristics of cluster B constructed of *M*-value profiles across eight binary comparisons of experimental conditions

Accession number	Sequence annotations – cluster B	GO terms-summary	Seq. clones	In cluster
*DQ847633	Cysteine proteinase preproenzyme	Cathepsin L	39	35
DQ847637	Cathepsin L	Cathepsin L	14	9
DQ847745	Digestive cysteine proteinase 3	Cathepsin L	4	1
DQ847747	Digestive cysteine proteinase 1	Cathepsin L	2	1
*DQ847749	Digestive cysteine proteinase 1	Cathepsin L	16	14
DQ847582	Cathepsin L	Cathepsin L		
DQ847591	Cysteine proteinase preproenzyme	Cathepsin L		
*DQ847755	Cathepsin L	Cathepsin L		
DQ847948	Digestive cysteine proteinase 2	Cathepsin L		
DQ847578	Trypsin	Trypsin		
DQ847600	Trypsin	Trypsin		
EF692624	Transmembrane serine protease 7	Trypsin	1	1
DQ847635	Trypsin	Trypsin		
DQ847976	Trypsin	Trypsin		
DQ847724	Triacylglycerol lipase	Lipid metabolism	11	6
DQ847596	Intracellular fatty acid binding protein	Lipid binding and transport		
DQ847606	Beta-1,4-endoglucanase	Cellulase		
DQ847628	Beta 1,4-endoglucanase	Cellulase		
DQ847699	Beta 1,4-endoglucanase	Cellulase		
*DQ847700	Beta 1,4-endoglucanase	Cellulase		
DQ847682	Alpha-L-fucoside fucohydrolase I	Carbohydrate metabolism		
DQ847632	Alpha-amylase	Carbohydrate metabolism		
DQ847892	Amylase I	Carbohydrate metabolism		
DQ847692	Peritrophic membrane chitin bindinprotein	Carbohydrate metabolism; hydrolase, acting on carbon-nitrogen nonpeptide bonds		
DQ847818	Chitinase	Extracellular chitinase		
DQ847963	Chitinase	Extracellular chitinase		
DQ847638	Chitinase	Chitin catabolism	11	1
DQ847757	(Q20AS9) ENSANGP00000021035-like	Chitin catabolism	2	1
DQ847845	(Q9VR69) CG32499-PA (RE51076p)	Chitin metabolism		
DQ847918	Cytochrome b	Mitochondrial		
DQ847538	NADH dehydrogenase subunit 3	Membrane NADH dehydrogenase (ubiquinone)		
DQ847742	NADH dehydrogenase subunit 1	Membrane NADH dehydrogenase (ubiquinone)		
DQ847754	NADH dehydrogenase subunit 1	Membrane NADH dehydrogenase (ubiquinone)		
DQ847575	NADH dehydrogenase subunit 2	Membrane NADH dehydrogenase (ubiquinone)		
DQ847649	NADH dehydrogenase subunit 6	Mitochondrial NADH dehydrogenase (ubiquinone)		
*DQ847740	RNA-dependent RNA polymerase	RNA-directed RNA polymerase; transcription		
*DQ847586	Haemocyanin	Oxygen transporter	13	11
DQ847608	Haemocyanin	Oxygen transporter		
*DQ847626	Haemocyanin	Oxygen transporter		
DQ847683	Haemocyanin	Oxygen transporter	7	2
DQ847639	(P83172) Haemocyanin C chain	Oxygen transporter		
DQ847695	Haemocyanin subunit 4 (hc4 gene)	Oxygen transporter		
DQ847688	Haemocyanin 2	Oxygen transporter	13	3
*DQ847739	Haemocyanin 2	Oxygen transporter		
DQ847704	Pseudohaemocyanin (PHc-1)		12	7
DQ847706	Pseudohaemocyanin (PHc-1)			
*DQ847595	Beta actin	Actin filament	8	3
DQ847651	Alpha actin			
*DQ847734	LOC443585 protein	Myosin; motor activity		
DQ847679	(Q6UDW6) Erythrocyte membrane protein 1		7	1
DQ847746	Antimicrobial peptide			
DQ847534	Elongation factor 1-alpha	Translational elongation factor		
EF692629	Elongation factor-1 alpha-like	Translational elongation factor	2	1
DQ847789	(Q56FK0) Ribosomal protein S23	Structural constituent of ribosome		
DQ847951	*Cherax* destructor ribosomal protein S18	Structural constituent of ribosome		
EF692613	Ribosomal protein l38e	Structural constituent of ribosome		
DQ847601	GA14025-PA			
DQ847619	PREDICTED: similar to DKFZP586A0522 protein			
DQ847959	(Q4DLB6) Putative mucin-associated surface protein (MASP)			
DQ847590	Ferritin peptide			
*DQ847866	*Triticum aestivum* clone wlsu2.pk0001.h3:fis			
*DQ847958	PREDICTED: similar to Clca1 protein			
DQ847756	(Q20AS9) ENSANGP00000021035-like			
EF426497	LEA dehydrin-like protein			
EF692594	Chromosome VII reading frame orf ygr108w			

Table 3. Continued

Accession number	Sequence annotations – cluster B	GO terms-summary	Seq. clones	In cluster
EF692600	Mgc81115 protein			
EF692604	*Procambarus clarkii* mRNA for complete cds			
EF692615	*Triticum aestivum* MADS-box transcription factor 16			
DQ847736	Cytochrome P450	Monooxygenase		
DQ847607	C-type lectin	Sugar binding		
EF692595	B-type cyclin involved in cell cycle progression	Regulation of cyclin-dependent protein kinase activity		
EF692605	*Drosophila melanogaster* cg14206	Cytoskeleton organization and biogenesis		
EF692607	Sallimus cg1915-isoform a	Cytoskeleton organization and biogenesis		
EF692610	*Solanum lycopersicum* clone: HTC in fruit	L-iditol 2-dehydrogenase activity		
EF692626	Leucyl-tRNA synthetases	Leucine-tRNA ligase activity		

Accession nos. of non-annotated unique clones: DQ847542; DQ847543; DQ847552; *DQ847599; DQ847620; DQ847631; *DQ847644; DQ847648; DQ847661; DQ847676; DQ847690; *DQ847693; *DQ847708; DQ847709; DQ847731; DQ847733; DQ847748; DQ847753; DQ847781; DQ847796; DQ847814; DQ847815; DQ847816; DQ847820; DQ847821; *DQ847822; DQ847824; DQ847855; DQ847859; *DQ847864; DQ847939; DQ847946; DQ847947; DQ847949; DQ847950; DQ847953; DQ847954; DQ847955; DQ847961; DQ847962; DQ847972; DQ847985; DQ847986; EF692585; EF692588; EF692590; EF692591; EF692597; EF692599; EF692608; EF692612; EF692614; EF692618; EF692627; EF692628

267 clones in cluster B, 22 of them were not sequenced — 154 unique clones in cluster B

Cluster B	Total DEC	Epre–Ref	Ipre–Ref	Epost–Ref	Ipost–Ref	Ipre–Ipost	Epre–Epost	Epre–Ipre	Epost–Ipost	ref 2-1	ref 3-1
DEC	233	147	215	155	180	22	14	33	1	6	12
Ave. *M* of DEC		–2.26 ± 0.74	–2.72 ± 1.08	–2.21 ± 0.75	–2.06 ± 0.82	–1.53 ± 0.63	1.62 ± 0.22	1.84 ± 0.95	–1.51	2.85 ± 0.32	1.32 ± 2.99

*The 18 highlighted accession numbers represent 33 differentially expressed unique clones in the Epre-Ipre binary comparison. See legend of Table 2.

Table 4. Characteristics of cluster C constructed of *M*-value profiles across eight binary comparisons of experimental condition

Accession number	Sequence annotations – cluster C	GO terms-summary	Seq. clones	In cluster
DQ847689	Hypothetical protein Bpse6_01003500		3	2
DQ847604	Mouse DNA sequence from clone RP23-56C2 on chromosome 2			
DQ847956	PREDICTED: similar to T-complex Chaperonin 5 CG8439-PA; isoform A			
DQ847633	Cysteine proteinase preproenzyme	Cathepsin L	39	1
EF692629	Elongation factor-1 alpha	Translational elongation factor	2	1
EF426497	LEA dehydrin-like protein			
EF692598	*Homo sapiens* chromosome 19 open reading frame 6 transcript variant mRNA			
DQ847679	(Q6UDW6) Erythrocyte membrane protein 1		7	1
DQ847965	*Cherax quadricarinatus* cytochrome *b*; mitochondrial gene and protein	Oxidoreductase		

Accession nos. of non-annotated unique clones: DQ847542; DQ847697; DQ847731; DQ847817; DQ847820; DQ847859; DQ847895; DQ847960; EF692586; EF692622

30 clones in cluster C, 1 of them were not sequenced — 20 unique clones in cluster C

Cluster C	Total DEC	Epre–Ref	Ipre–Ref	Epost–Ref	Ipost–Ref	Ipre–Ipost	Epre–Epost	Epre–Ipre	Epost–Ipost	ref 2-1	ref 3-1
DEC	20	8	9	10		18	20		2	1	1
Ave. *M* of DEC		1.39 ± 0.28	1.28 ± 0.23	–1.34 ± 0.25		1.53 ± 0.27	2.02 ± 0.32		–1.08 ± 0.05	–2.83	–3.04

See legend of Table 2.

these endoglucanases belong to a single gene, previously characterized in *C. quadricarinatus* (Byrne *et al*., 1999).

The single triacylglycerol lipase (DQ847724) was better represented in cluster B (6 of 11 clones) than in cluster A (2 of 11 clones).

Haemocyanins are a family of multi-functional crustacean proteins thought to be responsible for oxygen transport, phenoloxidase and antimicrobial activities, cross-linking of the initially flexible new exoskeleton after molting, and exoskeleton repair (reviewed in Terwilliger *et al*., 2006). There were three types of annotated haemocyanins in the present clusters: haemocyanin, haemocyanin 2 and pseudohaemocyanin. The pseudohaemocyanin does not have a heme prosthetic group, and is therefore not involved in oxygen transport. Haemocyanin and pseudohaemocyanin are represented mainly in cluster B while haemocyanin 2 is represented in cluster A, genuinely assigning them to the respective clusters.

Different unique chitinase and chitin metabolism-related sequences are present in clusters A (DQ847757), B (DQ847692; DQ847818; DQ847963; DQ847638; DQ847757; DQ847845), D (DQ847638) and F (DQ84618). DQ847638

Table 5. Characteristics of cluster D constructed of *M*-value profiles across eight binary comparisons of experimental conditions

Accession number	Sequence annotations – cluster D	GO terms-summary	Seq. clones	In cluster
DQ847612	Copper-specific metallothionein-2	Metal ion binding		
DQ847638	Chitinase	Chitin catabolism	11	6
Accession nos. of non-annotated unique clones	DQ847605; DQ847630; DQ847675; DQ847698; DQ847854; DQ847967; EF692609; EF692620			

19 clones in cluster D, four of them were not sequenced — 14 unique clones in cluster D

Cluster D	Total DEC	Epre–Ref	Ipre–Ref	Epost–Ref	Ipost–Ref	Ipre–Ipost	Epre–Epost	Epre–Ipre	Epost–Ipost	ref 2-1	ref 3-1
DEC	16	16	12	1		9	9				
Ave. *M* of DEC		–1.33 ± 0.53	–1.37 ± 0.47	–1.28		–1.19 ± 0.59	–1.28 ± 0.46				

See legend of Table 2.

Table 6. Characteristics of cluster E constructed of *M*-value profiles across eight binary comparisons of experimental conditions

Accession number	Sequence annotations – Cluster E	GO terms-summary	Seq. clones	In cluster
DQ847679	(Q6UDW6) Erythrocyte membrane protein 1		7	1
DQ847595	Beta actin	Actin filament	8	5
DQ847683	Haemocyanin	Oxygen transporter	7	1
EF692606	Elongation factor 1 gamma	Translation elongation factor		
Accession nos. of non-annotated unique clones		DQ847690; DQ847733; DQ847887; EF692597; EF692599; EF692616		

17 clones in cluster E, 3 of them were not sequenced — 13 unique clones in cluster E

Cluster E	Total DEC	Epre–Ref	Ipre–Ref	Epost–Ref	Ipost–Ref	Ipre–Ipost	Epre–Epost	Epre–Ipre	Epost–Ipost	ref 2-1	ref 3-1
DEC	10			7	6	2	6				
Ave. *M* of DEC				–1.25 ± 0.49	–0.83 ± 0.24	0.83 ± 0.03	1.28 ± 0.47				

See legend of Table 2.

Table 7. Characteristics of cluster F constructed of *M*-value profiles across eight binary comparisons of experimental conditions

Accession number	Sequence annotations – Cluster F	GO terms-summary	Seq. clones	In cluster
DQ847618	Chitinase 1	Extracellular chitinase		
DQ847688	Haemocyanin 2	Oxygen transporter	13	1
DQ847704	Pseudohaemocyanin (PHc-1)		12	1
DQ847971	Beta 1,4-endoglucanase	Cellulase	1	1
EF692587	Ribosomal protein s25	Structural constituent of ribosome		
Accession nos. of non-annotated unique clones	DQ847614; DQ847620; DQ847643; DQ847715; DQ847727; DQ847895; DQ847964; DQ847968; EF692589; EF692601; EF692625			

29 clones in cluster F, 11 of them were not sequenced — 27 unique clones in cluster F

Cluster F	Total DEC	Epre–Ref	Ipre–Ref	Epost–Ref	Ipost–Ref	Ipre–Ipost	Epre–Epost	Epre–Ipre	Epost–Ipost	ref 2-1	ref 3-1
DEC	15	1	1	10	10	12	13				
Ave. *M* of DEC		–1.88	–1.15	1.47 ± 0.67	1.2 ± 0.39		–1.51 ± 0.54	–1.75 ± 0.9			

See legend of Table 2.

genuinely belongs to cluster D, being much more abundant there. According to their annotations and the literature (Watanabe *et al.*, 1996; Tan *et al.*, 2000; Wang *et al.*, 2004), these unique clones probably belong to more than one gene. Tan *et al.* (2000) reported an increase in hepatopancreatic chitinase 1 expression levels concurrent with the peak of 20E, results that do not concur with those of the present study.

Five unannotated unique clones (DQ847542, DQ847543, DQ847648, DQ847661, DQ847708) also exhibited conflicting expression patterns in clusters A and B.

Quantitative PCR validation of microarray results

Validation of the microarray results was accomplished by binary comparisons of the relative expression levels of selected unique clones in selected experimental conditions, accomplished by quantitative relative real-time PCR. Combined equalized hepatopancreatic RNA populations of the XO-SG extirpated males at postmoult, injected males at premoult and intermoult males, were reverse transcribed and used as real-time PCR templates. Relative expression of the target genes of extirpated-postmoult, injected-postmoult

Table 8. Fold-expression of selected treated vs. control unique clones evaluated by both relative real time PCR and microarray analysis

Accession number	Cluster	Gene description	PCR primer pair	ΔCP (Ipre–Ref)	ΔCP (Epost–Ref)	ΔCP (Ipost–Ref)	*M*-value
DQ847728	Normalizing agent	18S RNA	F: CCTTCGCACGGTCAAAATACC R: AGTCTGACCTGCCCATTGGG	−0.1	−0.4	−0.6	–
*DQ847529	A	No annotation	F: TGAACACAGTTTCCACCATCG R: CTTGTATTGCACAGAATGCCC			1.28	–2.4
*DQ847688	A	Haemocyanin 2	F: TGAACTTGCCGTGAGGATCACC R: TGAATCTTCTGCATACAGCGCC		–5.6		1.46
DQ847716	A	No annotation	F: CCCATCATTGCCATAGTGTATGC R: ATCGCTCATTCAAACATTGTGC			1.95	1.84
DQ847751	A	No annotation	F: GGGCAGTTGACTTGTCTATTGGG R: CCTACCTGAAAACTCCGCATCC			0.5	1.65
DQ847643	A, D	No annotation	F:TTATAGCTGTTGGTCGCGTGG R: GTGATAAGGGAGCAGCTGAAGC		2.96		3.4
DQ847749	B	Digestive cysteine proteinase 1	F: TCTGGCCATGAACAAGTTTGC R: TGACTTGGTAGACGGTGTGGG	−4.37			−4.12
DQ847635	B	Trypsin	F: TGAGGGAGGAAAGGACTCTTGC R: CGTAACCCCAAGACACGATGC	–7.49			–5.09
DQ847818	B	Chitinase	F: ACACAACCAAGGATGACCAGTGG R: GGTCATGGCACCCAGTAGATGC	–1.66			–3.16
DQ847706	B	Pseudohaemocyanin (PHc-1)	F: GAAACCATTGTCAAGGTCTTCAACC R: GCACTTGTTTCTGTTAATGGTGACG		−4.43		−4.03
DQ847580	No cluster	No annotation	F: TGAACTTGCCGTGAGGATCACC R: TGAATCTTCTGCATACAGCGCC	2.82			1.62

*Conflicting real time PCR and microarray fold expressions.

Ref, intermoult males; Ipre, 20E-exposed males sacrificed at premoult; Epost, extirpated XO-SG males, sacrificed at postmoult; Ipost, 20E-exposed males sacrificed at postmoult. ΔCP, the difference between crossing-point real-time PCR cycles of the two RNA populations compared. *M*-value – $\log_2$ fold expression estimates derived from the microarray results.

and injected-premoult males vs. the intermoult males were semi-quantitatively evaluated by measuring the respective changes in crossing points (ΔCPs) (see 'Experimental procedures' below). The results are presented in Table 8, where they are compared to the respective microarray *M*-values. Both *M*-values and ΔCPs represent $\log_2$ fold-expression between the compared RNA populations, and although evaluated by different methods, they can be qualitatively compared, demonstrating similar expression trends in both analyses, excluding two unique clones (DQ847529 and DQ847688). The expression levels compared were normalized to total RNA and validated by the resulting, almost identical 18S RNA in the various RNA populations (ΔCPs of −0.1, −0.6 and −0.4 of treated relative to intermoult males, Table 8).

Discussion

A multi-gene approach aimed at identifying genes putatively involved in the moulting process was applied here for the first time in crustaceans. As the hepatopancreas is the major crustacean storage and metabolic organ, it was hypothesized that patterns of gene expression in this organ would change during the moult cycle. Support for this hypothesis was obtained from the results of Bielefeld *et al*. (1986) who studied hepatopancreatic moult-related transcript and protein expression profiles of the crayfish *Astacus leptodactylus*. Indeed, gene expression patterns related to the intermoult–premoult, and premoult–postmoult transitions were identified and characterized in the present study. The two measures of induction elucidated only a minor difference in gene expression patterns, and only at premoult.

The unique clone-specific data detailed above elucidated several apparently conflicting gene expression patterns. These incompatibilities are considered by us an inherent feature of cDNA microarrays, explained by the technical characteristics of this platform that must be considered when interpreting the biological significance of the results. Duplicates of the same clone were highly correlated. Hence, the reason for the *M*-value discrepancies between clones sharing the same accession number, as well as the lack of hybridization to part of the clones that share the same sequence, may be explained by parameters related to clones and their printing. Possible parameters include cDNA concentration in different clones, or the printing process itself, as different spots were printed with different printing tips. Furthermore, a shared accession number does not necessarily mean that the entire sequence is found in all the related clones, as partially overlapping sequences were assembled to a single unique clone. Cross-gene hybridization of genes belonging to the same family may further complicate the analysis because of their sequence similarities. More detailed discussions of sequence-related parameters affecting cross-gene DNA hybridization to spotted cDNAs as a possible source of

false positive signals can be found in Wren *et al*. (2002), Flikka *et al*. (2004), and Chen *et al*. (2006).

Consequently, hybridization results should be viewed as a sorting method for biologically interesting genes, the expressions of which should be further validated by sequencing and comparing full length cDNAs of gene family members. This allows the decisive determination of the number of gene members of each family in the array and also enables the design of gene-specific primer pairs for distinguishing expression levels via real-time PCR. However, hybridization is an efficient tool to reveal multigene expression patterns and their alterations with changing conditions.

The validation accomplished by real-time PCR showed a general agreement with the unique clone expression levels, elucidated by microarray hybridizations. A comparison of the two conflicting real-time PCR results with the microarray *M*-values may be explained by primers that share sequences with several differently expressed genes. One of them, DQ847688, annotated as haemocyanin 2, shared the sequence of at least one primer with other haemocyanins having different patterns of expression.

Cluster A is assumed to contain genes that are required for maintenance of the moult cycle. On average, however, it exhibited only a mild, two-fold induction. In addition the cysteine proteases, haemocyanin, pseudohaemocyanin, endoglucanase and triacylglycerol lipase mostly genuinely assigned to cluster B (see results above). Therefore, only glutamine synthetase can be interpreted at present as a moult-maintaining enzyme. Elucidating the role of induced haemocyanin 2 requires further analysis in comparison with other haemocyanins, which are located in cluster B.

Cluster B is assumed to comprise genes and pathways that are attenuated throughout the premoult and early postmoult periods. Many of them are metabolic enzymes, proteases, endoglucanase, lipases and carbohydrate metabolism-related enzymes. Other attenuated transcripts belong to the mitochondrial energy-providing pathways (NADH dehydrogenase subunits). Taken together, these instances of reduced transcription indicate a reduced hepatopancreas metabolic rate. The reduction of haemocyanin is puzzling because one expects that during moult there would be a greater need for oxygen. Alternatively, haemocyanin 2 may fulfil this requirement. Hepatopancreatic chitinases and chitin metabolism-related genes probably function as digestive enzymes for ingested chitin, therefore, fit to cluster B, of attenuated unique clones. However, additional functions related to digestion of endogenic chitin during premoult may be hypothesized, assigning others to clusters A, D and F. The present variety of partial cDNAs related to chitin metabolism may serve as a basis for more detailed study of this important metabolic system in arthropods.

Although moulting is common to all arthropods, being driven by the same moulting hormone, it is difficult to compare existing insect studies to the present study, as none of the insect expression patterns was examined in a metabolic organ comparable to the hepatopancreas. However, the concurrent accumulation of crustacean sequence and microarray-related data and the corresponding insect information may enable future identification of specific genes and gene families, evolutionary-related within two taxa and demonstrating similar or diversifying expression patterns and functions.

We are aware of the fact that some of the altered genes may result from stress, caused by the XO-SG extirpation or by the repeated injections.

Immediate future research directions benefiting from this study include: (1) distinguishing among the structures and functions of annotated genes belonging to the same gene family (e.g. haemocyanins, chitinases, endoglucanases and proteases); (2) complete sequencing of differentially expressed non-annotated genes, which may lead to further annotations; (3) comparing the present expression patterns with those of tissues directly involved in the moulting process, such as the epidermis and the Y organ; and (4) studying the regulation mechanisms of the general transcription pattern shift of the hepatopancreas upon entering premoult.

To summarize, the present study provides a microarray tool for sorting expression gene patterns in *C. quadricarinatus* tissues. The moulting induction experiment sorted putative hepatopancreatic transcripts participating in the moulting process. The partial sequences of annotated and novel genes and their assigned expression patterns may provide a basis for more detailed studies.

Experimental procedures

Materials

The stock solution for preparing various dilutions of saline sodium citrate (SSC) was 20 × SSC (3 M NaCl, 0.3 M sodium citrate, pH 7.4). Total RNA extraction from crayfish tissues was performed using the EZ-RNA II (Biological Industries, Beit Haemek, Israel) and RNeasy (Qiagen, Valencia, CA, USA) kits. The PolyTtract kit (Promega, Madison, WI, USA) was used for mRNA extraction from total RNA solutions. SMART and PCR-select kits (Clontech, Mountain View, CA, USA) were used to construct equalized cDNA assemblages for spotting on the microarray slides. Cloning of cDNAs into plasmid vectors was carried out with the pGEM-T easy kit (Promega), and Taq polymerase (Sigma, St Louis, MO, USA; # D1806) was used for PCR amplification of cDNA clones for spotting on a microarray slide. Real-time PCR utilized moloney murine leukemia virus (MMLV) reverse transcriptase (Promega, # M1701) and real time SYBR green mix ×2 (Finnzymes, Finland, #F-410). Components of the labelling protocol of hybridized cDNAs included the reverse transcriptase ImProm II (Promega #A3802), amino allyl-dUTP (Ambion, Austin, TX, USA #8439) and Cy3 and Cy5 mono-reactive succinimidyl ester-derivatized NHS-ester fluorescent dyes (Amersham PA23001 and PA25001 for Cy3 and Cy5,

respectively; Amersham, Piscataway, NJ, USA). Each tube of dry dye was dissolved in 72 μl of dimethyl sulfoxide (DMSO) and divided into eight aliquots. At several stages of the labelling process, Qiaquick kit (Qiagen) was used to extract cDNAs.

Preparation of cDNA microarray

Cherax quadricarinatus males to be used for preparation of the cDNA assemblage were maintained in 700-L containers at a temperature of 28 °C under natural light, and fed *ad libitum* with wheat grains and ground carrot and potatoes. The XO-SG complex was bilaterally extirpated from six males, after which they were kept in separate cages. These animals were then sacrificed at 13 or 14 days post-extirpation, and weighed. Several hepatopancreatic lobes, epidermal layers beneath the carapace, muscle tissue and the entire Y organ pair were dissected out of each sacrificed male. The sampled tissues were immediately snap-frozen in liquid nitrogen. The gastroliths were also removed and weighed and premoult specimens having gastrolith indexes >1.5–2.5 [gastrolith weight/body weight; mg/g] characteristic of premoult (Tom & Dauphin-Villemant, unpublished data) and setae development characteristic of premoult individuals (Shechter *et al*., 2007) were identified. RNA was extracted from the dissected tissues of premoult males using a commercial kit (RNeasy, Qiagen). Hepatopancreas, epidermis and Y-organs served as target tissues, and muscle as the reference tissue.

The cDNA assemblage was constructed in two stages: (1) switching mechanism at 5′ end of the RNA transcript (SMART)-based amplification of reverse-transcribed cDNAs using a universal primer linked to both ends of the template cDNA during the reverse transcription stage (Clontech, manufacturer's instructions); and (2) subtractive-suppression hybridization (SSH) method-based T-A cloning of roughly equally represented cDNAs from the target organs, into an expression plasmid. The SSH method was designed to prefer differentially expressed genes in the target tissues relative to the reference tissue (Diatchenko *et al*., 1999; PCR-select, Clontech). Furthermore, a complementary SSH process, which involves switching the target and reference tissues to reveal additional transcripts present in the reference tissue but reduced in the target tissue, is usually performed. However, this procedure is beneficial only when the same tissue, sampled under two biological situations, serves as both reference and target tissue. Our cDNA assemblage was prepared against a reference tissue, *C. quadricarinatus* muscle, in which we had no biological interest in the context of this study. The resulting cDNA population was actually a wide transcript assemblage originating from our target tissues, presumably biased only against general housekeeping genes expressed in all *C. quadricarinatus* tissues. The cloned cDNAs were transfected into *Escherichia coli*, and 4800 bacterial colonies were isolated, amplified and frozen at –80 °C. A subset of the clones were sequenced and assembled by CAP3 software (Huang & Madan, 1999) to identify unique clones.

All 4800 clones were amplified by standard PCR from 1 μl of bacterial culture templates (5 min at 95 °C; 32 cycles of 0.5 min at 95 °C, 0.5 min at 68 °C, and 1.5 min at 72 °C; a final incubation of 4 min at 72 °C; GeneAmp 5700, Applied Biosystems, Foster City, CA, USA). PCR products were precipitated from the PCR solution by one volume of isopropanol at room temperature. The dry DNA was dissolved in a printing buffer at a final concentration of 50% DMSO and 0.3 × SSC and amplification efficiency was tested by running the PCR products on a 1% agarose gel with a DNA mass ladder, then printing the products on a glass slide (GAPS II slides, Corning Life Sciences, Lowell, MA, USA; BioRobotics MicroGrid, Genomic Solutions, Ann Arbor, MI, USA) in duplicates. The printing pattern included two complete and separate sets of the transcriptome in the upper and lower parts of the slide, respectively.

Moult induction experiment

Before and during the experiment, *C. quadricarinatus* males were maintained in captivity at 28 °C with a photoperiod of 14L : 10D (Parnes & Sagi, 2002). Male crayfish intended for the moult induction experiment were divided into two groups, one subjected to XO-SG extirpation, and the other to multiple 20E injections. In each of these two treatment groups, three animals were sacrificed at the premoult stage and three others a day after ecdysis. Both interventions were performed according to Shechter *et al*. (2007). The moult stage was monitored throughout the experiment by a non-invasive X-ray examination. In addition, haemolymph samples of 100 μl were withdrawn each day and stored, and ecdysteroid levels were determined later according to Shechter *et al*. (2007). The experiment was terminated by immersing the crayfish in ice-cold water for several minutes for anaesthesial metabolism reduction, after which they were sacrificed. Weight and carapace length were recorded for each individual, as was the setae development index of moult stage (Shechter *et al*., 2007). The hepatopancreas was dissected out and immediately divided into several pieces, which were snap-frozen in liquid nitrogen and stored at –80 °C. Total RNA and mRNA were purified later from the frozen tissue. Their amount was evaluated by spectrophotometry at 260 nm and their quality was tested by their 260/280 nm absorbance ratio and their electrophoretic profiles on 1% agarose gel, generally according to Sambrook & Russell (2001) and using commercial kits when appropriate.

Hybridization procedure

Messenger RNA populations extracted from treated and reference hepatopancreatic tissues were labelled with the fluorescent dyes Cy3 and Cy5 by using the amino-allyl indirect cDNA labelling method as follows: 200–400 ng of mRNA of the transcript population was incubated for 10 min at 70 °C with 100 μg dT primer ($T_{15}VN$) and immediately chilled on ice. The resulting RNA-dT primer hybrid was reverse transcribed in a total volume of 30 μl for 1 h at 42 °C in a solution containing reverse transcriptase (1.5 μl/reaction), 32 units of RNase inhibitor, 3.5 mM of $MgCl_2$ solution and 0.5 mM dNTP mix in which the dTTP had been replaced by an amino allyl-dUTP/dTTP mixture (4 : 1). Reverse transcription was followed by mRNA hydrolysis for 15 min at 65 °C at an alkaline pH [0.2 M NaOH (fresh), and 0.1 M of EDTA]. The alkaline solution was neutralized with 0.35 M HEPES buffer (pH 7.0), followed by buffer replacement and cDNA concentration, performed by washing the solution three times with 450 μl of water through a Microcon YM-30 filter (Amicon, #8439, Millipore, Billerica, MA, USA). The final solution volume was between 50–100 μl. The cDNAs were coupled to an aliquot of the Cy3 or Cy5 mono-reactive succinimidyl ester-derivatized NHS-ester fluorescent dye via the reactive amino allyl groups. The reaction was carried out for 1 h at room temperature in 9 μl of 0.1-M fresh Na-bicarbonate buffer, pH 9.0. Hydroxylamine was added to the solution at a final concentration of 1.33 M and the solution was incubated for 15 min at room temperature. Finally, the solution was neutralized with sodium acetate pH 5.2, to a final concentration of 72 mM and purified with an affinity column-based kit (Qiaquick, Qiagen). Labelling efficiency was evaluated by

spectrophotometry at 260 nm for cDNA estimation and 550 nm (Cy3) and 650 nm (Cy5) for determining labelling intensity.

Microarray slides were incubated with a pre-hybridization solution [1% bovine serum albumin; 5× SSC; 0.1% sodium dodecylsulphate (SDS), 25% formamide] for 2 h at 42 °C to block nonspecific DNA interactions, thus reducing background fluorescence. This step was followed by two short rinses in water, one rinse in ethanol and drying by mild centrifugation of vertical slides. Dual-labelled solutions for binary comparisons between the two experimental conditions were prepared by mixing the two labelled cDNA populations to be compared, followed by a 1:1 dilution with a hybridization solution containing 200 μg/ml salmon sperm DNA, 10× SSC, 0.2% SDS and 50% formamide. The heat denatured hybridization mixture (3 min at 95 °C) was layered onto the microarray, covered (Lifterslip, Erie Scientific, Portsmouth, NH, USA; #25x60-2-4789), and incubated overnight at 42 °C in a humidified hybridization chamber (Corning). Following incubation, the slides were washed as follows: 5 min at 42 °C in 2× SSC – 0.1% SDS, mild shaking for 10 min at room temperature in 0.1× SSC – 0.1% SDS; mild shaking 4 × 5 min at room temperature in 0.1× SSC, followed by two quick dips, one in water and one in ethanol. The slides were dried by centrifugation and scanned by a GenePix 4000B scanner at two wavelengths corresponding to the Cy3 and Cy5 emissions. The dual fluorescence images were quantified by the *GENEPIX* software (Molecular Devices, Sunnyvale, CA, USA), which also provided a weight index evaluating the quality of each hybridized spot.

Design and analysis of the hybridized slides

Individual variability, an important biological factor, was automatically integrated into the hybridization design by using the RNA populations of three individual crayfish from each experimental condition (Epost, Ipost, Epre and Ipre; see key to designations in the results section above and legends of Tables 2–7). The three reference groups comprised RNA of six individuals (Ref1) and three each from Ref2 and Ref3. Three hybridization sets were performed, each composed of eight slides. In each set, one individual from each treatment was compared to one of the reference pools, and, in addition, the treated individuals were compared to each other, as detailed in Fig. 1A. The design was balanced with respect to the dye labelling of the RNA populations, such that each individual RNA population was labelled with one dye on one slide and with the other dye in two other slides (arrow directions in Fig. 1A). To evaluate the variability between the three reference RNA populations, an additional hybridization set of three slides was carried out with the reference pools as shown in Fig. 1B.

Data analysis was conducted with the *R* computational environment (http://www.r-project.org/), using *BioConductor* software packages (Gentleman *et al*., 2005). Initially, the *ArrayQuality* package was used to assess the quality of the hybridizations according to the software user's manual, and malfunctioned hybridizations were repeated.

The calculation and statistical analysis of $\log_2$ expression ratios for each clone in a binary comparison was carried out using the *LIMMA* package (Linear Models for Microarray data Analysis; Smyth, 2004, 2005). *GENEPIX* quantified image files were imported into *LIMMA* and spots which agreed to *GENEPIX* quality criteria were used. The Cy5 and Cy3 intensities within each slide were normalized using the print-tip locally weighted scatter plot smoothing (LOESS) method, while no background correction was applied. For each spot on an individual slide, *LIMMA* calculated an *M*-value [$M = (\log_2(\text{Cy5})/\text{Cy3})$; Cy5 and Cy3 are the normalized emission intensities of the spot] and an emission intensity *A* value [$A = (\log_2(\text{Cy5}) * \text{Cy3})/2$]. Subsequently, *LIMMA* fitted a linear model to the expression data followed by empirical Bayes smoothing. The inter-duplicate correlation method was used at the linear modelling step. The mean-*A* values, representing the average spot emission intensities across the analysed experiment, were also calculated. Only spots fulfilling mean-$A > 8.5$ were included in the subsequent analysis, thus avoiding faint emissions.

For each clone, the *LIMMA* summary statistics included an estimated average *M*-value across each binary comparison associated with two statistical parameters: the *B* statistic, the log-odds that the spot was differentially expressed, and the *P*-value, which was derived from a moderated *t*-statistic after multiple testing corrections according to Benjamini & Hochberg (1995). Clones were considered differentially expressed between two experimental conditions within a binary comparison when both $P < 0.05$ and $B > 1.5$ were met.

The *M*-value profiles of all analysed clones across the eight selected binary comparisons were arranged in a *spot x M*-value matrix and clustered using *EXPANDER* software, which contains a battery of adjustable clustering methods (Sharan *et al*., 2003; http://www.cs.tau.ac.il/~rshamir/expander/expander.html). The following clustering algorithms were used: *Click* with homogeneity values of 0.85, 0.9 and nonspecified homogeneity, *K*-means with 6–10 predetermined numbers of clusters, and *SOM* using 2 × 2, 2 × 3 and 3 × 3 matrices. Eventually, biologically relevant clusters, which corresponded to the aims of the induction experiment were selected. The *M*-values of redundant clones belonging to the same unique clone were averaged within each cluster.

Sequenced clones belonging to each of the selected clusters were annotated using both the BLASTX and BLASTN algorithms (Altschul *et al*., 1997). When available, GO annotations (Ashburner *et al*., 2000) were borrowed from the BLAST hits. Both sequence and GO annotations were attained using the BLAST2GO software (http://www.blast2go.de/; Conesa *et al*., 2005). Only BLAST hits with *e*-values $< 10^{-5}$ and their derived GO terms were considered valid annotations.

Quantitative relative real-time PCR

The relative expression levels of target transcripts from the two compared *C. quadricarinatus* RNA populations were evaluated using reverse transcription coupled with relative real-time PCR, according to Pfaffl (2001). A RNA mix was created from equally pooled RNAs of the three individuals comprising each experimental condition, and aliquots of 1, 0.5, 0.25 and 0.125 μg total RNA of each mix were reverse transcribed at 42 °C for 1 h using suitable reverse primers, according to Sambrook & Russell (2001). PCR reactions were performed for selected target genes, and also for the 18S RNA, using the four reverse transcriptase solutions of each RNA population as templates. Each reaction was performed in triplicate with the GeneAmp 5700 PCR thermocycler (Applied Biosystems, Foster City, CA, USA) (one cycle at 50 °C, 2 min; one cycle at 95 °C, 10 min; 40 cycles at 95 °C, 15 s and 60 °C, 1 min). A standard PCR reaction was conducted with a volume of 25 μl composed of 12.5 μl SYBR Green mix, 0.2 μM of each of the PCR primers, and a 2 μl aliquot sample from the reverse transcription mixture.

A linear regression equation relating the crossing-point (CP) of the PCR cycle to the log of the four dilutions was calculated for each PCR-reacted RNA population. The equation slope was used to ensure a reasonably similar PCR efficiency of the two RNA populations compared. A semiquantitative evaluation of relative

expression was calculated from the ΔCP between the two RNA populations compared and was normalized to spectrophotometrically evaluated total RNAs.

Acknowledgements

The study was partially supported by the U.S.–Israel Binational Science Foundation (grant nos. 97-288 and 2000116) and by the Israel Science Foundation grant no. 1080/05. Thanks are due to M. Maria Sigal for her excellent care of the crayfish, Ms Meirav Segev and Dr Eduard Yakubov for their assistance in the preparation of the cDNA transcriptome; Dr Miriam Kott-Gutkowski from the Faculty of Medicine, The Hebrew University of Jerusalem is thanked for provision of slide-related services; and Mr Patrick Martin for editorial review of the manuscript.

References

Abdu, U., Davis, C., Khalaila, I. and Sagi, A. (2002) The vitellogenin cDNA of *Cherax quadricarinatus* encodes a lipoprotein with calcium binding ability, and its expression is induced following the removal of the androgenic gland in a sexually plastic system. *Gen Comp Endocrinol* **127**: 263–272.

Aiken, D.E. and Waddy, S.L. (1987) Molting and growth in crayfish, a review. *Can Tech Rep Fish Aquat Sci* **1587**: 1–34.

Altschul, S.F., Madden, T.L., Schäffer, A.A., Zhang, J., Zhang, Z., Miller, W. *et al*. (1997) Gapped BLAST and PSI-BLAST: a new generation of protein database search programs. *Nucleic Acids Res* **25**: 3389–3402.

Arbeitman, M.N., Furlong, E.E.M., Imam, F., Johnson, E., Null, B.H., Baker, B.S. *et al*. (2002) Gene expression during the life cycle of *Drosophila melanogaster*. *Science* **297**: 2270–2275.

Ashburner, M., Ball, C.A., Blake, J.A., Botstein, D., Butler, H., Cherry, J.M. *et al*. (2000) Gene ontology: tool for the unification of biology. *Nature Genet* **25**: 25–29.

Barki, A., Levi, T., Hulata, G. and Karplus, I. (1997) Annual cycle of spawning and molting in the red-claw crayfish, *Cherax quadricarinatus*, under laboratory conditions. *Aquaculture* **157**: 239–249.

Beckstead, R.B., Lam, G. and Thummel, C.S. (2005) The genomic response to 20-hydroxyecdysone at the onset of *Drosophila* metamorphosis. *Genome Biol* **6 R99**: 13.

Benjamini, Y. and Hochberg, Y. (1995) Controlling the false discovery rate: a practical and powerful approach to multiple testing. *J Royal Stat Soc Ser B* **57**: 289–300.

Bielefeld, M., Gellissen, G. and Spindler, K.D. (1986) Protein production and the moulting cycle in the crayfish *Astacus leptodactylus*. *J Insect Biochem* **16**: 175–180.

Byrne, K.A., Lehnert, S.A., Johnson, S.E. and Moore, S.S. (1999) Isolation of a cDNA encoding a putative cellulase in the red claw crayfish *Cherax quadricarinatus*. *Gene* **239**: 317–324.

Chang, E.S. (1991) Crustacean molting hormones, cellular effects, role in reproduction and regulation by molt inhibiting hormone. In *Frontiers of Shrimp Research* (Deloach, P.F., Dougherty, W.J. and Davidson, M.A., eds), pp. 83–106. Elsevier Science Publishers, Amsterdam.

Chang, E.S. (1995) Physiological and biochemical changes during the molt cycle in decapod crustaceans: an overview. *J Exp Mar Biol Ecol* **193**: 1–14.

Chang, E.S., Bruce, M.J. and Tamone, S.L. (1993) Regulation of crustacean molting-a multi-hormonal system. *Am Zool* **33**: 324–329.

Chen, Y., Chou, C.-C., Lu, X., Slate, E., Peck, K., Xu, W., *et al*. (2006). A multivariate prediction model for microarray cross-hybridization. *BMC Bioinformatics* **7**: 101.

Conesa, A., Gotz, S., Garcia-Gomez, J.M., Terol, J., Talon, M. and Robles, M. (2005) Blast2GO: a universal tool for annotation, visualization and analysis in functional genomics research. *Bioinformatics* **21**: 3674–3676.

Dell, S., Sedlmeier, D., Boecking, D. and Dauphin-Villemant, C. (1999) Ecdysteroid biosynthesis in crayfish Y-organs: Feedback regulation by circulating ecdysteroids. *Arch Insect Biochem Physiol* **41**: 148–155.

Dhar, A.K., Dettori, A., Roux, M.M., Klimpel, K.R. and Read, B. (2003) Identification of differentially expressed genes in shrimp (*Penaeus stylirostris*) infected with white spot syndrome virus by cDNA microarrays. *Arch Virol* **148**: 2381–2396.

Diatchenko, L., Lukyanov, S., Lau, Y.F.C. and Siebert, P.D. (1999) Suppression subtractive hybridization: a versatile method for identifying differentially expressed genes. In cDNA Preparation and Characterization, *Meth Enzymol* **303**: 349–380. Academic Press Inc, San Diego, CA.

Flikka, K., Yadetie, F., Laegreid, A. and Jonassen, I. (2004) XHM: A system for detection of potential cross hybridizations in DNA microarrays. *BMC Bioinformatics* **5**: 117.

Gentleman, R., Carey, V.J., Huber, W., Irizarry, R.A. and Dudoit, S. (eds) (2005) *Bioinformatics And Computational Biology Solutions Using R and Bioconductor. Statistics for Biology and Health*. Springer, New York, NY.

Glenner, H., Thomsen P.F., Hebsgaard, M.B., Sørensen M.V. and Willerslev E. (2007) The origin of insects. *Science* **314**: 1883–1884.

Goodisman, M.A.D., Isoe, J., Wheeler, D.E. and Wells, M.A. (2005) Evolution of insect metamorphosis: a microarray-based study of larval and adult gene expression in the ant *Camponotus festinatus*. *Evolution* **59**: 858–870.

Huang, X. and Madan, A. (1999) CAP3: A DNA sequence assembly program. *Gen Res* **9**: 868–877.

Keller, R., (1992) Crustacean neuropeptides – structures, functions and comparative aspects. *Experientia* **48**: 439–448.

Lachaise, F., Leroux, A., Hubert, M. and Lafont, R. (1993) The molting gland of crustaceans – localization, activity, and endocrine control (a review). *J Crust Biol* **13**: 198–234.

Le Boulay, C., Van Wormhoudt, A. and Sellos, D. (1995) Molecular cloning and sequencing of two cDNAs encoding cathepsin L-related cysteine proteinases in the nervous system and in the stomach of the Norway lobster (*Nephrops norvegicus*). *Comp Biochem Physiol* **111**: 353–359.

Nelson, K. (1991) Scheduling of reproduction in relation to molting and growth in malacostracan crustaceans. In *Crust Issues* (Wenner, A. and Kuris, A., eds), Vol. 7, pp. 77–113. A. Balkema, Rotterdam, the Netherlands; Brookfield, Vermont, USA.

Ote, M., Mita, K., Kawasaki, H., Seki, M., Nohata, J., Kobayashi, M., *et al*. (2004) Microarray analysis of gene expression profiles in wing discs of *Bombyx mori* during pupal ecdysis. *Insect Biochem Mol Biol* **34**: 775–784.

Parnes, S. and Sagi, A. (2002) Intensification of redclaw crayfish *Cherax quadricarinatus* culture – I. Hatchery and nursery system. *Aquacult Engineer* **26**: 251–262.

Pfaffl, M.W. (2001) A new mathematical model for relative quantification in real-time RT-PCR. *Nucleic Acids Res* **29**: 2003–2007.

Sambrook, J. and Russell, D.W. (2001) *Molecular Cloning, A Laboratory Manual*, 3rd edn. Cold Spring Harbor Laboratory Press, Cold Spring Harbor, NY.

Sharan, R., Maron-Katz, A. and Shamir, R. (2003) CLICK and EXPANDER, a system for clustering and visualizing gene expression data. *Bioinformatics* **19**: 1787–1799.

Shechter, A., Tom, M., Yudkovski, Y., Weil, S., Chang S.A., Chang E.S., *et al*. (2007) On the search for hepatopancreatic ecdysone-responsive genes during the crayfish molt cycle: from a single gene to multigenicity. *J. Exp. Biol.* (in press).

Skinner, D.M. (1962). The structure and metabolism of a crustacean integumentary tissue during a molt cycle. *Biol Bull* **123**: 635–647.

Skinner, D.M. (1985) Molting and regeneration. In *The Biology of Crustacea*, Vol. 9 (Bliss, D.E. and Mantel, L.H., eds), pp. 43–146. Academic Press, New York.

Smyth, G.K. (2004) Linear models and empirical bayes methods for assessing differential expression in microarray experiments. *Stat Appl Genet Mol Biol* **3** (1): Article 3. http://www.bepress.com/sagmb/vol3/iss1/art3.

Smyth, G.K. (2005) LIMMA: linear models for microarray data. In *Bioinformatics and Computational Biology Solutions Using R and Bioconductor. Statistics for Biology and Health* (Gentleman, R., Carey, V.J., Huber, W., Irizarry, R.A. and Dudoit, S., eds), pp. 397–420. Springer, New York, NY.

Soetaert, A., Moens, L.N., Van der Ven, K., Van Leemput, K., Naudts, B., Blust, R., *et al*. (2006) Molecular impact of propiconazole on *Daphnia magna* using a reproduction-related cDNA array. *Comp Biochem Physiol C-Toxicol Pharmacol* **142**: 66–76.

Stepanyan, R., Day, K., Urban, J., Hardin, D.L., Shetty, R.S., Derby, C.D., *et al*. (2006) Gene expression and specificity in the mature zone of the lobster olfactory organ. *Physiol Genom* **25**: 224–233.

Stillman, J.H., Teranishi, K.S., Tagmount, A., Lindquist, E.A., Brokstein, P.B. and Stillman, A.F. (2006) Construction and characterization of EST libraries from the porcelain crab, *Petrolisthes cinctipes*. *Integrat Comp Biol* **46**: 919–930.

Stringfellow, L.A. and Skinner, D.M. (1988) Molt-cycle correlated patterns of synthesis of integumentary proteins in the land crab *Gecarcinus lateralis*. *Dev Biol* **128**: 97–110.

Tan, S.H., Degnan, B.M. and Lehnert, S.A. (2000) The *Penaeus monodon* chitinase 1 gene is differentially expressed in the hepatopancreas during the molt cycle. *Mar Biotechnol* **2**: 126–135.

Terwilliger, N.B., Ryan, M. and Phillips, M.R. (2006) Crustacean hemocyanin gene family and microarray studies of expression change during eco-physiological stress. *Integrat Comp Biol* **46**: 991–999.

Traub, M., Gellissen, G. and Spindler, K.D. (1987) 20 (OH) ecdysone induced transition from intermolt to premolt protein biosynthesis patterns in the hypodermis of the crayfish, *Astacus leptodactylus in vitro*. *Gen Comp Endocrinol* **65**: 469–477.

Wang, P., Li, G. and Granados, R.R. (2004) Identification of two new peritrophic membrane proteins from larval *Trichoplusia ni*: Structural characteristics and their functions in the protease rich insect gut. *Insect Biochem Mol Biol* **34**: 215–227.

Watanabe, T., Kono, M., Aida, K. and Nagasawa, H. (1996) Isolation of cDNA encoding a putative chitinase precursor in the kuruma prawn *Penaeus japonicus*. *Mol Marine Biol Biotechnol* **5**: 299–303.

White, K.P., Rifkin, S.A., Hurban, P and Hogness, D.S. (1999) Microarray analysis of *Drosophila* development during metamorphosis. *Science* **286**: 2179–2184.

Wren, J., Kulkarni, A., Joslin, J., Butow, R. and Garner, H. (2002). Cross-hybridization on PCR-spotted microarrays. *IEEE Eng Med Biol Mag* **21**: 71–75.